Int. J. Mol. Sci. **2013**, *14*, 14700-14711; doi:10.3390/ijms140714700

OPEN ACCESS

International Journal of

Molecular Sciences

ISSN 1422-0067

www.mdpi.com/journal/ijms

Article

Enhanced Development of Azoxymethane-Induced Colonic Preneoplastic Lesions in Hypertensive Rats

Takahiro Kochi [1], Masahito Shimizu [1,*], Tomohiko Ohno [1], Atsushi Baba [1], Takafumi Sumi [1], Masaya Kubota [1], Yohei Shirakami [1], Hisashi Tsurumi [1], Takuji Tanaka [2] and Hisataka Moriwaki [1]

[1] Department of Internal Medicine, Gifu University Graduate School of Medicine, Gifu 501-1194, Japan; E-Mails: kottii924@yahoo.co.jp (T.K.); tomohikooh@hotmail.com (T.O.); babagif@yahoo.co.jp (A.B.); sumieron@gmail.com (T.S.); kubota-gif@umin.ac.jp (M.K.); shirakamiyy@yahoo.co.jp (Y.S.); htsuru@gifu-u.ac.jp (H.T.); hmori@gifu-u.ac.jp (H.M.)

[2] Department of Tumor Pathology, Gifu University Graduate School of Medicine, Gifu 501-1194, Japan; E-Mail: takutt@toukaisaibou.co.jp

* Author to whom correspondence should be addressed; E-Mail: shimim-gif@umin.ac.jp; Tel.: +81-58-230-6313; Fax: +81-58-230-6310.

Received: 2 May 2013; in revised form: 25 June 2013 / Accepted: 27 June 2013 / Published: 15 July 2013

Abstract: Metabolic syndrome is associated with an increased risk of colorectal cancer. This study investigated the impact of hypertension, a component of metabolic syndrome, on azoxymethane (AOM)-induced colorectal carcinogenesis using SHRSP/Izm (SHRSP) non-diabetic/hypertensive rats and SHRSP.Z-*Lepr*^{fa}/IzmDmcr (SHRSP-ZF) diabetic/hypertensive rats. Male 6-week-old SHRSP, SHRSP-ZF, and control non-diabetic/normotensive Wister Kyoto/Izm (WKY) rats were given 2 weekly intraperitoneal injections of AOM (20 mg/kg body weight). Two weeks after the last injection of AOM, the SHRSP and SHRSP-ZF rats became hypertensive compared to the control WKY rats. Serum levels of angiotensin-II, the active product of the renin-angiotensin system, were elevated in both SHRSP and SHRSP-ZF rats, but only the SHRSP-ZF rats developed insulin resistance, dyslipidemia, and hyperleptinemia and exhibited an increase in adipose tissue. The development of AOM-induced colonic preneoplastic lesions and aberrant crypts foci, was significantly accelerated in both SHRSP and SHRSP-ZF hypertensive rats, compared to WKY normotensive rats. Furthermore, induction of oxidative stress and exacerbation of inflammation were observed in the colonic mucosa and systemically in SHRSP and SHRSP-ZF rats. Our findings suggest that hypertension plays a role in the early

stage of colorectal carcinogenesis by inducing oxidative stress and chronic inflammation, which might be associated with activation of the renin-angiotensin system.

Keywords: hypertension; colon carcinogenesis; oxidative stress; inflammation; angiotensin-II

1. Introduction

Obesity-related systemic metabolic dysfunctions such as diabetes mellitus, hypertension, and dyslipidemia are collectively known as metabolic syndrome (Mets) and pose serious health problems throughout the world [1,2]. In addition to the morbidity associated with these metabolic disorders, recent studies have revealed that Mets is linked to an increased risk of cancer in several organ sites including the colorectum [3–8]. Several pathophysiological mechanisms for this association have been described, including the emergence of insulin resistance, the state of chronic inflammation, induction of oxidative stress, and occurrence of adipokine imbalance [5,6]. In particular, diabetes is closely associated with the development of colorectal cancer (CRC) as obesity is the main determinant of insulin resistance and hyperinsulinemia [7].

Epidemiological studies have also revealed that hypertension may increase the risk of CRC [3,4]. The renin-angiotensin system is a key regulator of cardiovascular function, and its activation is involved in the etiology of Mets, especially hypertension [9]. There is increasing evidence that the renin-angiotensin system may have paracrine and autocrine functions with regard to tissue oxidative stress and chronic inflammation, as well as cellular proliferation and apoptosis [10–14]. In addition, dysregulation of the renin-angiotensin system has been reported to occur in human malignancies and has been shown to influence cancer cell migration, invasion, and metastasis, all of which are associated with a poor prognosis [10,11,14]. However, the precise mechanisms by which hypertension plays a role in the early stage of colorectal carcinogenesis remain unclear.

The stroke-prone spontaneously hypertensive rat (SHRSP) is a substrain of the spontaneously hypertensive rat (SHR), crossed and further inbred with selected offspring of parents that died of stroke. The SHRSP rats have a higher blood pressure than SHR rats and readily develop apoplexy. The crossing of SHRSP rats with Zucker Fatty (ZF) rats produces SHRSP.*Z-Lepr*^{fa}/IzmDmcr (SHRSP-ZF) rats, which develop hypertension and become obese due to the leptin receptor *OB-rb* gene mutation carried by ZF rats [15]. SHRSP-ZF rats therefore exhibit a phenotype similar to human Mets and thus may be a useful model to investigate the molecular mechanisms underlying hypertension-related metabolic abnormalities [15,16]. However, colorectal carcinogenesis models using these rats have not been established.

The objective of this study was to determine the susceptibility of SHRSP-ZF and SHRSP rats to azoxymethane (AOM)-induced colorectal carcinogenesis and the utility of these rats as models for Mets, in particular, as models for hypertension-associated colorectal carcinogenesis, that appropriately reflect the pathological conditions of human Mets.

2. Results and Discussion

2.1. General Observations

Table 1 compares the mean body weights, adipose tissue weights, and blood pressures (systolic and diastolic) at the end of the study (10 weeks of age) between 3 groups (Group 1, Wister Kyoto/Izm [WKY] rats; Group 2, SHRSP rats; and Group 3, SHRSP-ZF rats) that received AOM. The mean body weights of WKY ($p < 0.001$) and SHRSP-ZF ($p < 0.05$) rats were significantly higher than that of SHRSP rats, but there was no significant difference between the WKY and SHRSP-ZF rats. There was a significant increase in the mean adipose tissue weights in SHRSP-ZF rats compared to WKY ($p < 0.001$) and SHRSP rats ($p < 0.05$). The systolic and diastolic blood pressures of SHRSP and SHRSP-ZF rats were markedly higher than those of WKY rats ($p < 0.001$). However, compared to SHRSP-ZF rats, SHRSP rats had marked hypertension ($p < 0.05$).

Table 1. Body, liver and adipose weights, BMI and blood pressure of rats.

Group NO.	Strain	No.	Body weight (g)	Relative adipose tissue weight (g/100g body weight) [a]	Blood pressure (mmHg)	
					Systolic	Diastolic
Group 1	WKY [b]	8	256.5 ± 11.7 [e]	0.72 ± 0.16	127 ± 12.8	92 ± 4.9
Group 2	SHRSP [c]	8	218.9 ± 8.0 [f]	0.77 ± 0.16	188 ± 12.5 [f]	141 ± 10.6 [f]
Group 3	SHRSP-ZF [d]	8	270.1 ± 23.4 [g]	1.64 ± 0.17 [f,g]	169 ± 13.7 [f,g]	129 ± 9.0 [f,g]

[a] White adipose tissue of the periorchis; [b] Wister Kyoto/Izm; [c] stroke-prone spontaneously hypertensive/Izm; [d] SHRSP.Z-*Leprfa*/IzmDmcr; [e] Mean ± SD; [f] Significantly different from group 1 by Tukey-Kramer Multiple Comparison Test ($p < 0.001$); [g] Significantly different from group 2 by Tukey-Kramer Multiple Comparison Test ($p < 0.05$).

2.2. Serum Parameters of the Experimental Rats

As shown in Table 2, the serum levels of glucose and insulin significantly increased, but the value of QUICKI, a useful index of insulin sensitivity [17], was decreased in SHRSP-ZF rats compared to WKY and SHRSP rats ($p < 0.05$). The serum levels of leptin, non-esterified fatty acid (NEFA), and triglycerides in SHRSP-ZF rats were also significantly higher than those in WKY and SHRSP rats ($p < 0.05$). These findings suggest that SHRSP-ZF rats developed insulin resistance, hyperleptinemia, and dyslipidemia, all of which are frequently observed in human Mets patients. There were no significant differences in these serum components between WKY and SHRSP rats. The SHRSP and SHRSP-ZF rats did, however, have significantly elevated levels of serum angiotensin-II (AT-II), the active product of the renin-angiotensin system [18], compared to the WKY rats ($p < 0.05$), indicating that the renin-angiotensin system is activated in these hypertensive rats.

Table 2. Serum parameters of the experimental rats.

	Glucose (mg/dL)	Insulin (μIU/mL)	Quicki	Leptin (pg/mL)	NEFA (mEq/L)	Triglyceride (mg/dL)	Angiotensin II (ng/mL)
Group 1	85.4 ± 11.7	15.81 ± 0.35	0.313 ± 0.010	11.2 ± 3.6	0.459 ± 0.03	27.1 ± 7.4	352.6 ± 38.1
Group 2	83.5 ± 12.3	17.00 ± 1.39	0.320 ± 0.008	12.2 ± 3.4	0.419 ± 0.05	39.6 ± 14.1	494.4 ± 75.6 [b]
Group 3	120.0 ± 14.2 [b,c]	25.60 ± 8.98 [b,c]	0.291 ± 0.010 [b,c]	102.7 ± 30.6 [b,c]	0.538 ± 0.03 [b,c]	257.1 ± 79.4 [b,c]	500.9 ± 42.5 [b]

[a] Mean ± SD; [b] Significantly different from group 1 by Tukey-Kramer Multiple Comparison Test ($p < 0.05$); [c] Significantly different from group 2 by Tukey-Kramer Multiple Comparison Test ($p < 0.05$).

2.3. Development of Colonic Preneoplastic Lesions

Irrespective of the rat strain, aberrant crypt foci (ACF) (Figure 1A) were observed in the colon of all rats given AOM at the end of the study. However, the number and size (aberrant crypts [ACs] per cm^2) of ACF were significantly greater in both the SHRSP and SHRSP-ZF rats than in the WKY rats (Figure 1B; $p < 0.05$). There was no significant difference in the development of ACF between SHRSP and SHRSP-ZF rats, indicating that hypertension, a common pathophysiological characteristic of these rats, plays a critical role in accelerating the development of colonic preneoplastic lesions.

Figure 1. ACF developed in the SHRSP, SHRSP-ZF, and WKY rats that received AOM. (**A**) Representative morphology of ACF (arrows) induced by AOM stained with methylene blue in Group 2. Magnification, 40×; (**B**) Average number of ACF and ACs (/cm^2). Group 1: WKY rats, Group 2: SHRSP rats, and Group 3: SHRSP-ZF rats. The values are expressed as mean ± SD. * $p < 0.05$.

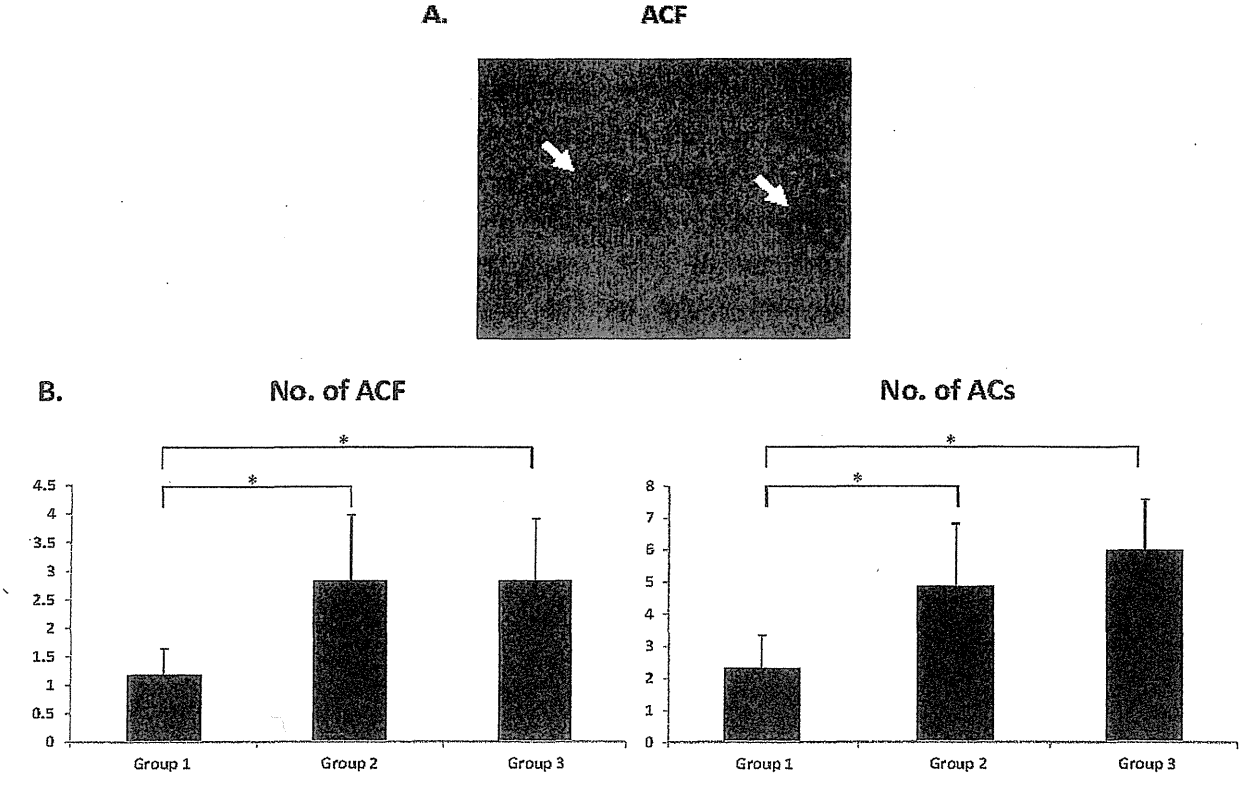

2.4. Systemic Oxidative Stress and Colonic Epithelial Expression of GPx and CAT mRNA

Oxidative stress is implicated in Mets and colorectal tumorigenesis [5]. Therefore, the levels of oxidative stress and antioxidant biomarkers in the experimental rats were assessed. Compared to the WKY rats, the SHRSP and SHRSP-ZF rats had significantly increased levels of urine 8-hydroxy-2'-deoxyguanosine (8-OHdG) (Figure 2A; $p < 0.01$), a marker of DNA damage induced by oxidative stress, and serum derivatives of reactive oxygen metabolites (d-ROM) (Figure 2B; $p < 0.01$), which reflects serum hydroperoxide levels. However, the SHRSP and SHRSP-ZF rats also had reduced expression levels of glutathione peroxidase (*GPx*) and catalase (*CAT*) mRNA, which encode antioxidant enzymes, in the colonic epithelium (Figure 2C; $p < 0.05$). These findings suggest that systemic oxidative stress is increased, whereas colonic antioxidant activity is decreased, in both SHRSP and SHRSP-ZF hypertensive rats.

Figure 2. Measures of oxidative stress and antioxidant biomarkers' expression. (**A**) Urine 8-OHdG levels were measured by enzyme immunoassay; (**B**) Hydroperoxide levels in the serum were determined by the d-ROM test; (**C**) The expression levels of *GPx* and *CAT* mRNA in the colonic epithelium were examined by quantitative real-time RT-PCR using specific primers. The values are expressed as mean ± SD. * $p < 0.01$, ** $p < 0.01$.

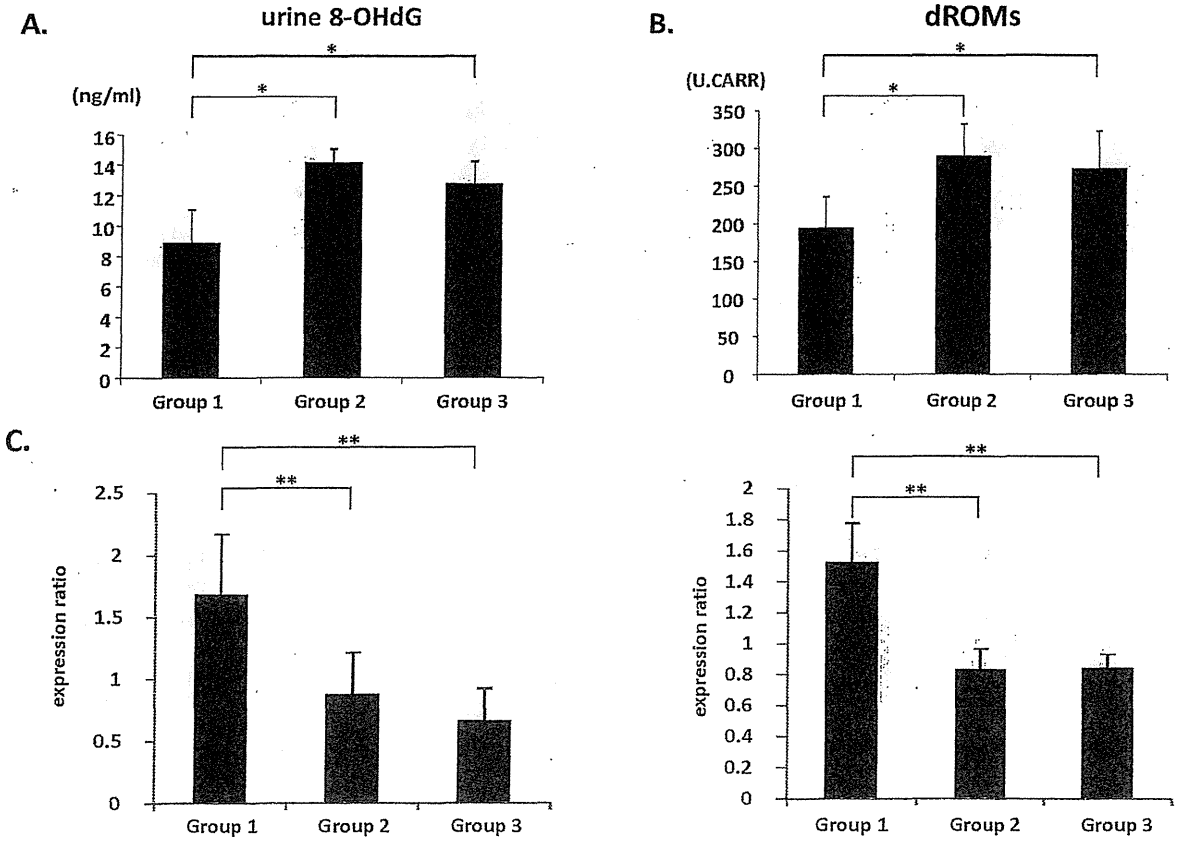

2.5. Serum and Colonic Epithelial Expression of Inflammatory Markers

Chronic inflammation plays a critical role in the pathogenesis of Mets and CRC development [5,8]. Therefore, the levels of inflammatory mediators, including tumor necrosis factor (TNF)-α, interleukin

(IL)-6, monocyte chemoattractant protein (MCP)-1, inducible nitric oxide synthase (iNOS), and cyclooxygenase (COX)-2 in hypertensive SHRSP and SHRSP-ZF rats were next examined. The serum levels of TNF-α and IL-6 in SHRSP-ZF rats were significantly elevated compared to those in WKY rats (Figure 3A; $p < 0.01$). The serum levels of COX-2 were also significantly increased in both SHRSP and SHRSP-ZF rats (Figure 3A; $p < 0.01$). In the colonic epithelium of SHRSP-ZF rats, there was a marked increase in the expression of *TNF-α*, *MCP-1*, and *iNOS* mRNA (Figure 3B; $p < 0.05$ compared to WKY rats). Compared to the WKY rats, the expression of *TNF-α* mRNA in the colonic epithelium of SHRSP rats was also significantly increased (Figure 3B; $p < 0.05$).

Figure 3. Serum levels of TNF-α, IL-6, and COX-2 and the expression levels of *TNF-α*, *MCP-1*, and *iNOS* mRNA in the colonic epithelium. (**A**) The serum concentrations of TNF-α, IL-6, and COX-2 were measured by enzyme immunoassay; (**B**) The expression levels of *TNF-α*, *MCP-1*, and *iNOS* mRNA in the colonic epithelium were examined by quantitative real-time RT-PCR using specific primers. The values are expressed as mean ± SD. * $p < 0.01$, ** $p < 0.05$.

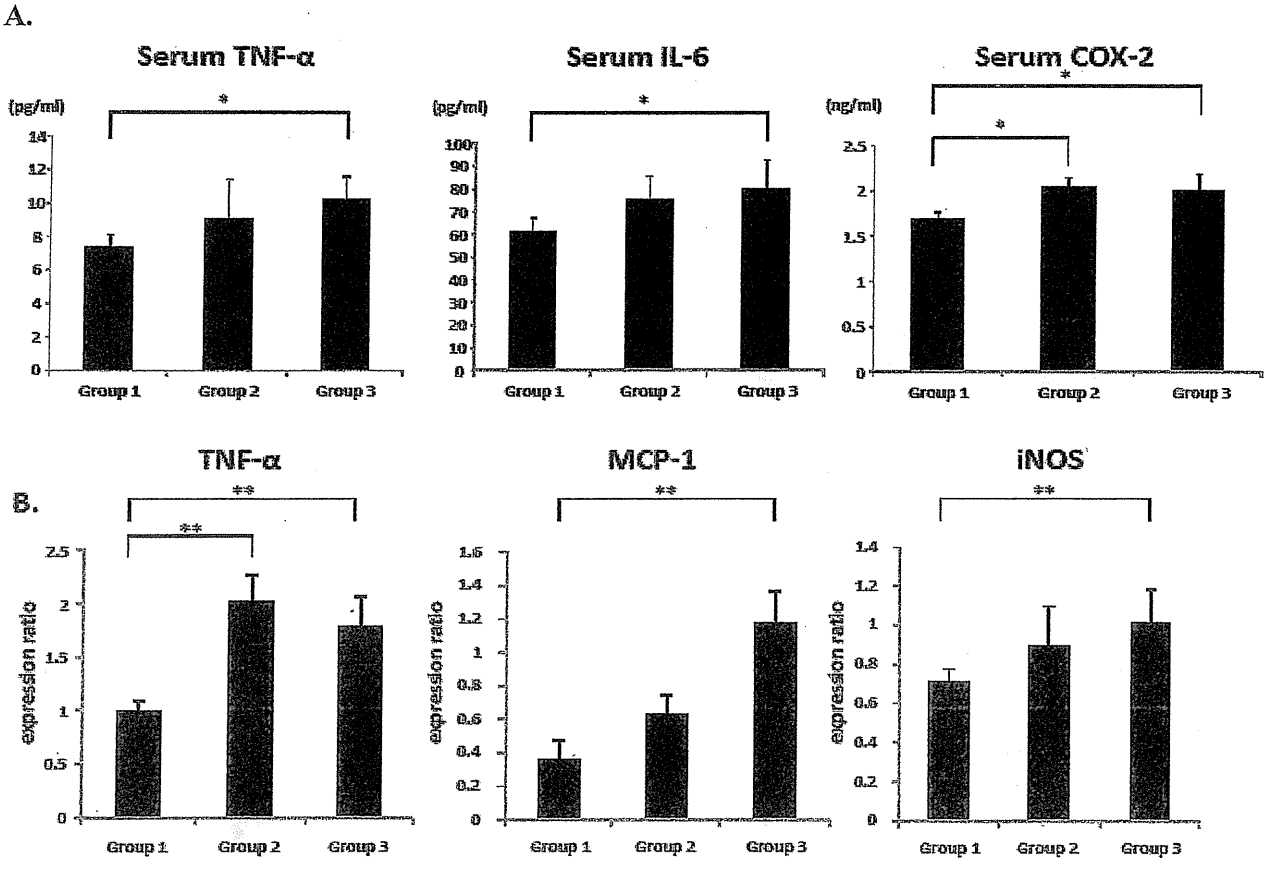

2.6. Discussion

Increasing evidence suggests that Mets is involved in the development of CRC, and this continues to be a growing health problem worldwide, especially in developed countries [1–5]. Recent epidemiological studies have suggested that patients with hypertension, a component of Mets [1,2], comprise a high-risk

group for CRC [3–5]. However, appropriate animal models to evaluate hypertension-related colorectal carcinogenesis have not yet been generated.

To our knowledge, the present study provides the first evidence that after administration of AOM, SHRSP and SHRSP-ZF rats, both of which present with hypertension, more readily develop colonic preneoplastic lesions than normotensive WKY rats. In particular, we found that SHRSP rats experience accelerated development of ACF. This is significant because these rats did not exhibit insulin resistance, hyperleptinemia, or dyslipidemia and did not have increased adipose tissue, which are involved in the pathophysiology thought to link Mets to CRC [5–8]. These findings, therefore, suggest that hypertension *per se* might play a critical role in the early events of colorectal carcinogenesis. We have found that the angiotensin converting enzyme inhibitor captopril, an anti-hypertensive drug, significantly prevents the development of ACF in SHRSP-ZF rats [19]. These findings also support our hypothesis that blood pressure elevation *per se* might be directly involved in the early stage of colorectal carcinogenesis. However, in order to test this hypothesis, further studies are needed to establish whether other anti-hypertensive agents, such as AT-II type 1 receptor blockers and calcium channel blockers, can suppress the development of ACF by lowering blood pressure.

Among the pathophysiological disorders associated with hypertension, an increased level of oxidative stress is thought to be particularly important in CRC development [5,6]. Oxidative stress, defined as the overproduction of oxygen species combined with inadequate anti-oxidative defense mechanisms, can result in DNA damage and, consequently, mutations associated with colorectal carcinogenesis [5,20]. In the present study, the hypertensive SHRSP and SHRSP-ZF rats had significantly elevated urine 8-OHdG levels and serum d-ROM levels, which are associated with increased oxidative stress [21]. However, they also had reduced *GPx* and *CAT* mRNA levels, both of which encode antioxidant enzymes, in the colonic epithelium. These findings indicate that both SHRSP and SHRSP-ZF rats are subjected to strong oxidative stress, which might contribute to the development of ACF.

In addition to oxidative stress, the induction of chronic inflammation is also considered to play a critical role in obesity-, diabetes-, and hypertension-related colorectal carcinogenesis [5,6]. In the present study, serum levels of TNF-α and IL-6, as well as colonic expression of *MCP-1* and *iNOS* mRNA, were markedly elevated in SHRSP-ZF obese and diabetic rats. These changes might have been associated with the increase in adipose tissue in SHRSP-ZF rats because excess adipose tissue plays an important role in the exacerbation of systemic inflammation [22,23]. Furthermore, colonic epithelial expression of *TNF-α* mRNA and serum levels of COX-2 were significantly higher in both the hypertensive SHRSP and SHRSP-ZF rats, although the former did not become obese or develop diabetes. These findings are also significant because the dysregulation of TNF-α, a central mediator of chronic inflammatory diseases, and COX-2 have key roles in the stimulation of tumor growth and the progression of carcinogenesis in several tissues, including the colon and rectum [24,25].

Why did the SHRSP rats, which did not exhibit obesity and insulin resistance, experience an acceleration of oxidative stress, exacerbation of chronic inflammation, and development of ACF to the same extent as SHRSP-ZF rats that are both obese and diabetic? One possible explanation is that the dose of AOM (20 mg/kg body weight) used in the present protocol was considerably greater than that needed to induce ACF development in these hypertensive rats. A lower dose of AOM may therefore result in differences in both the number and size of ACF between SHRSP and SHRSP-ZF rats. It is also possible that an increase in the serum level of AT-II, which is the main effector peptide of the

renin-angiotensin system [12,13], might contribute to these phenomena because renin-angiotensin system activation has been implicated in the increase in oxidative stress and the induction of inflammation [11,14,26,27]. Renin-angiotensin system activation induces adipocyte inflammation, as demonstrated by the increased expression of TNF-α and IL-6 in adipose tissue, which in turn is implicated in hypertension [28,29]. In prostate cancer, treatment with AT-II stimulates the secretion of IL-6 and MCP-1 from prostate stromal cells and is associated with the increased proliferation of prostate cancer cells [30]. AT-II also induces the expression of iNOS, an inflammatory marker, along with 8-OHdG in prostate cancer cells [31], suggesting a crosslink between renin-angiotensin system-related inflammation and oxidative stress in cancer tissue.

To date, there is no definitive evidence demonstrating the effectiveness of renin-angiotensin system inhibitors in preventing human malignancies, including CRC, in hypertensive patients [32–35]. However, our findings suggest that targeting hypertension-related metabolic abnormalities, including oxidative stress and chronic inflammation caused by renin-angiotensin system activation, may be an effective strategy to prevent CRC development in patients with Mets, especially those with hypertension. In malignant tissue such as CRC, dysregulation of the renin-angiotensin system is implicated in cancer cell migration, invasion, and metastasis [10,11,13,14,36]. A recent study also showed that treatment with renin-angiotensin system inhibitors could inhibit chemically induced colorectal carcinogenesis in obese and diabetic mice by attenuating chronic inflammation and oxidative stress [37]. In order to test the potential efficacy of renin-angiotensin system inhibitors in preventing CRC development in patients with Mets, additional long-term experiments to evaluate whether these agents can prevent colorectal carcinogenesis in hypertensive rats should be conducted.

3. Experimental Section

3.1. Animals and Chemicals

Five-week-old male SHRSP, SHRSP-ZF, and WKY rats were obtained from Japan SLC (Shizuoka, Japan) and humanely maintained at Gifu University Life Science Research Center in accordance with the Institutional Animal Care Guidelines. The WKY rats are normotensive and not prone to obesity, and thus served as the control group in this study. AOM, which is widely used to mimic sporadic colon carcinogenesis by causing DNA mutations and activating several oncogenic pathways, including the K-*ras* pathway [38,39], was purchased from Wako (Osaka, Japan).

3.2. Experimental Procedure

After 1 week of acclimatization, the 6-week-old rats were divided into 3 groups of 8 rats each. All rats received an intraperitoneal injection of AOM (20 mg/kg body weight) once a week for 2 weeks. The experimental protocol and dose of AOM were based on previous studies using F344, Sprague-Dawley, or Wister rat strains [40,41]. We did not include non-AOM treated WKY rats as negative controls because no ACF was found to develop in these animals in a preliminary experiment. At the end of the experiment (2 weeks after the last injection of AOM), when the rats were 10 weeks of age, systolic and diastolic blood pressures were measured noninvasively using a tail cuff (SOFTRON BP98A; Softron, Tokyo, Japan). All rats were euthanized by CO_2 asphyxiation for colon resection. The third portion of

the excised colons (cecum side) was used to extract RNA, and the remaining part was used to determine the number of ACF [42].

3.3. Enumeration of ACF

The frequency of AOM-induced colonic premalignant lesions, ACF, was determined as previously described [42]. Briefly, the colon samples were fixed with 10% buffered formalin, stained with methylene blue (0.5% in distilled water) for 20 s, and then placed on microscope slides to count the number of ACF. The number of ACF was recorded along with the number of ACs in each focus. The data are expressed per unit area (cm^2).

3.4. RNA Extraction and Quantitative Real-Time Reverse Transcription-Polymerase Chain Reaction Analysis

The epithelial crypts were isolated from colonic tissue [41]. Total RNA was then extracted from the isolated epithelial crypts using the RNAqueous-4PCR kit (Ambion Applied Biosystems, Austin, TX, USA). cDNA was amplified from 0.2 μg of total RNA using the SuperScript III First-Strand Synthesis System (Invitrogen, Carlsbad, CA, USA). Quantitative real-time reverse transcription-PCR (RT-PCR) analysis was performed using specific primers that amplify *TNF-α*, *MCP-1*, *iNOS*, *GPx*, *CAT*, and glyceraldehyde-3-phosphate dehydrogenase (*GAPDH*) genes. The sequences of these primers, which were obtained from Primer-BLAST [43], are listed in Table S1. Each sample was analyzed on a LightCycler Nano (Roche Diagnostics, Basel, Switzerland) using FastStart Essential DNA Green Master (Roche Diagnostics). Parallel amplification of *GAPDH* was used as the internal control.

3.5. Clinical Biochemistry

Blood samples from the inferior vena cava were used for chemical analyses. These samples were obtained at the time of euthanasia, prior to which the rats had fasted for 6 h. The serum levels of TNF-α (R&D Systems, Minneapolis, MN, USA), IL-6 (R & D Systems), insulin (Shibayagi, Gunma, Japan), glucose (BioVision Research Products, Mountain View, CA, USA), leptin (Shibayagi), triglyceride (Wako), NEFA (Wako), AT-II (Phoenix Pharmaceuticals, INC, Burlingame, CA, USA), and COX-2 (MyBioSource, San Diego, CA, USA) were determined using an enzyme-linked immunosorbent assay (ELISA) kit according to the manufacturer instructions.

3.6. Oxidative Stress Analysis

Urine 8-OHdG levels were determined using an ELISA kit (NIKKEN SEIL, Shizuoka, Japan). Serum levels of hydroperoxide, a marker for oxidative stress, were evaluated using the d-ROM test (FREE Carpe Diem; Diacron s.r.l., Grosseto, Italy) [21].

3.7. Statistical Analysis

All data are presented as mean ± SD and were analyzed using the GraphPad InStat software program version 3.05 (GraphPad Software, San Diego, CA, USA) for Macintosh. One-way analysis of variance

(ANOVA) was used to compare groups. If the ANOVA analysis indicated significant differences, the Tukey-Kramer multiple comparisons test was performed to compare the mean values among the groups. The differences were considered significant when the two-sided p value was less than 0.05.

4. Conclusions

The results of this study indicate that the development of AOM-induced colonic preneoplastic lesions was significantly accelerated in hypertensive rats compared to normotensive rats. This was associated with hypertension-related renin-angiotensin system activation and subsequent induction of oxidative stress and inflammation, suggesting that hypertension plays a critical role in the early stages of CRC.

Conflict of Interest

The authors declare no conflict of interest.

References

1. Alberti, K.G.; Zimmet, P.; Shaw, J.; IDF Epidemiology Task Force Consensus Group. The metabolic syndrome—A new worldwide definition. *Lancet* **2005**, *366*, 1059–1062.
2. Grundy, S.M.; Cleeman, J.I.; Daniels, S.R.; Donato, K.A.; Eckel, R.H.; Franklin, B.A.; Gordon, D.J.; Krauss, R.M.; Savage, P.J.; Smith, S.C., Jr.; *et al.* Diagnosis and management of the metabolic syndrome: An American Heart Association/National Heart, Lung, and Blood Institute Scientific Statement. *Circulation* **2005**, *112*, 2735–2752.
3. Ahmed, R.L.; Schmitz, K.H.; Anderson, K.E.; Rosamond, W.D.; Folsom, A.R. The metabolic syndrome and risk of incident colorectal cancer. *Cancer* **2006**, *107*, 28–36.
4. Stocks, T.; van Hemelrijck, M.; Manjer, J.; Bjorge, T.; Ulmer, H.; Hallmans, G.; Lindkvist, B.; Selmer, R.; Nagel, G.; Tretli, S.; *et al.* Blood pressure and risk of cancer incidence and mortality in the Metabolic Syndrome and Cancer Project. *Hypertension* **2012**, *59*, 802–810.
5. Ishino, K.; Mutoh, M.; Totsuka, Y.; Nakagama, H. Metabolic syndrome: A novel high-risk state for colorectal cancer. *Cancer Lett.* **2012**, doi:10.1016/j.canlet.2012.10.01.
6. Shimizu, M.; Kubota, M.; Tanaka, T.; Moriwaki, H. Nutraceutical approach for preventing obesity-related colorectal and liver carcinogenesis. *Int. J. Mol. Sci.* **2012**, *13*, 579–595.
7. Yuhara, H.; Steinmaus, C.; Cohen, S.E.; Corley, D.A.; Tei, Y.; Buffler, P.A. Is diabetes mellitus an independent risk factor for colon cancer and rectal cancer? *Am. J. Gastroenterol.* **2011**, *106*, 1911–1921.
8. Donohoe, C.L.; Pidgeon, G.P.; Lysaght, J.; Reynolds, J.V. Obesity and gastrointestinal cancer. *Br. J. Surg.* **2010**, *97*, 628–642.
9. De Kloet, A.D.; Krause, E.G.; Woods, S.C. The renin angiotensin system and the metabolic syndrome. *Physiol. Behav.* **2010**, *100*, 525–534.
10. Ager, E.I.; Neo, J.; Christophi, C. The renin-angiotensin system and malignancy. *Carcinogenesis* **2008**, *29*, 1675–1684.
11. Deshayes, F.; Nahmias, C. Angiotensin receptors: A new role in cancer? *Trends Endocrinol. Metab.* **2005**, *16*, 293–299.

12. Paul, M.; Poyan Mehr, A.; Kreutz, R. Physiology of local renin-angiotensin systems. *Physiol. Rev.* **2006**, *86*, 747–803.
13. Fyhrquist, F.; Saijonmaa, O. Renin-angiotensin system revisited. *J. Intern. Med.* **2008**, *264*, 224–236.
14. George, A.J.; Thomas, W.G.; Hannan, R.D. The renin-angiotensin system and cancer: Old dog, new tricks. *Nat. Rev. Cancer* **2010**, *10*, 745–759.
15. Hiraoka-Yamamoto, J.; Nara, Y.; Yasui, N.; Onobayashi, Y.; Tsuchikura, S.; Ikeda, K. Establishment of a new animal model of metabolic syndrome: SHRSP fatty (fa/fa) rats. *Clin. Exp. Pharmacol. Physiol.* **2004**, *31*, 107–109.
16. Ueno, T.; Takagi, H.; Fukuda, N.; Takahashi, A.; Yao, E.H.; Mitsumata, M.; Hiraoka-Yamamoto, J.; Ikeda, K.; Matsumoto, K.; Yamori, Y. Cardiovascular remodeling and metabolic abnormalities in SHRSP.Z-Lepr(fa)/IzmDmcr rats as a new model of metabolic syndrome. *Hypertens. Res. Off. J. Jpn. Soc. Hypertens.* **2008**, *31*, 1021–1031.
17. Chen, H.; Sullivan, G.; Yue, L.Q.; Katz, A.; Quon, M.J. QUICKI is a useful index of insulin sensitivity in subjects with hypertension. *Am. J. Physiol. Endocrinol. Metab.* **2003**, *284*, E804–E812.
18. Chrysant, S.G.; Chrysant, G.S.; Chrysant, C.; Shiraz, M. The treatment of cardiovascular disease continuum: Focus on prevention and RAS blockade. *Curr. Clin. Pharmacol.* **2010**, *5*, 89–95.
19. Kochi, K.; Shimizu, M.; Ohno, T.; Baba, A.; Sumi, T.; Kubota, M.; Shirakami, Y.; Tsurumi, H.; Tanaka, T.; Moriwaki, H. Department of Internal Medicine, Gifu University Graduate School of Medicine, 2013, Unpublished data.
20. Tudek, B.; Speina, E. Oxidatively damaged DNA and its repair in colon carcinogenesis. *Mutat. Res.* **2012**, *736*, 82–92.
21. Suzuki, Y.; Imai, K.; Takai, K.; Hanai, T.; Hayashi, H.; Naiki, T.; Nishigaki, Y.; Tomita, E.; Shimizu, M.; Moriwaki, H. Hepatocellular carcinoma patients with increased oxidative stress levels are prone to recurrence after curative treatment: A prospective case series study using the d-ROM test. *J. Cancer Res. Clin. Oncol.* **2013**, in press.
22. Hotamisligil, G.S.; Shargill, N.S.; Spiegelman, B.M. Adipose expression of tumor necrosis factor-alpha: Direct role in obesity-linked insulin resistance. *Science* **1993**, *259*, 87–91.
23. Hotamisligil, G.S. Inflammation and metabolic disorders. *Nature* **2006**, *444*, 860–867.
24. Szlosarek, P.; Charles, K.A.; Balkwill, F.R. Tumour necrosis factor-alpha as a tumour promoter. *Eur. J. Cancer* **2006**, *42*, 745–750.
25. Gupta, R.A.; Dubois, R.N. Colorectal cancer prevention and treatment by inhibition of cyclooxygenase-2. *Nat. Rev. Cancer* **2001**, *1*, 11–21.
26. Cassis, P.; Conti, S.; Remuzzi, G.; Benigni, A. Angiotensin receptors as determinants of life span. *Pflugers Arch.* **2010**, *459*, 325–332.
27. Smith, G.R.; Missailidis, S. Cancer, inflammation and the AT1 and AT2 receptors. *J. Inflam.* **2004**, *1*, 3.
28. Massiera, F.; Bloch-Faure, M.; Ceiler, D.; Murakami, K.; Fukamizu, A.; Gasc, J.M.; Quignard-Boulange, A.; Negrel, R.; Ailhaud, G.; Seydoux, J.; *et al.* Adipose angiotensinogen is involved in adipose tissue growth and blood pressure regulation. *FASEB* **2001**, *15*, 2727–2729.
29. Yvan-Charvet, L.; Massiera, F.; Lamande, N.; Ailhaud, G.; Teboul, M.; Moustaid-Moussa, N.; Gasc, J.M.; Quignard-Boulange, A. Deficiency of angiotensin type 2 receptor rescues obesity but not hypertension induced by overexpression of angiotensinogen in adipose tissue. *Endocrinology* **2009**, *150*, 1421–1428.

30. Uemura, H.; Ishiguro, H.; Nagashima, Y.; Sasaki, T.; Nakaigawa, N.; Hasumi, H.; Kato, S.; Kubota, Y. Antiproliferative activity of angiotensin II receptor blocker through cross-talk between stromal and epithelial prostate cancer cells. *Mol. Cancer Ther.* **2005**, *4*, 1699–1709.
31. Uemura, H.; Ishiguro, H.; Ishiguro, Y.; Hoshino, K.; Takahashi, S.; Kubota, Y. Angiotensin II induces oxidative stress in prostate cancer. *Mol. Cancer Res. MCR* **2008**, *6*, 250–258.
32. Lever, A.F.; Hole, D.J.; Gillis, C.R.; McCallum, I.R.; McInnes, G.T.; MacKinnon, P.L.; Meredith, P.A.; Murray, L.S.; Reid, J.L.; Robertson, J.W. Do inhibitors of angiotensin-I-converting enzyme protect against risk of cancer? *Lancet* **1998**, *352*, 179–184.
33. Lang, L. ACE inhibitors may reduce esophageal cancer incidence. *Gastroenterology* **2006**, *131*, 343–344.
34. Sipahi, I.; Chou, J.; Mishra, P.; Debanne, S.M.; Simon, D.I.; Fang, J.C. Meta-analysis of randomized controlled trials on effect of angiotensin-converting enzyme inhibitors on cancer risk. *Am. J. Cardiol.* **2011**, *108*, 294–301.
35. Hallas, J.; Christensen, R.; Andersen, M.; Friis, S.; Bjerrum, L. Long term use of drugs affecting the renin-angiotensin system and the risk of cancer: A population-based case-control study. *Br. J. Clin. Pharmacol.* **2012**, *74*, 180–188.
36. Shimomoto, T.; Ohmori, H.; Luo, Y.; Chihara, Y.; Denda, A.; Sasahira, T.; Tatsumoto, N.; Fujii, K.; Kuniyasu, H. Diabetes-associated angiotensin activation enhances liver metastasis of colon cancer. *Clin. Exp. Metast.* **2012**, *29*, 915–925.
37. Kubota, M.; Shimizu, M.; Sakai, H.; Yasuda, Y.; Ohno, T.; Kochi, T.; Tsurumi, H.; Tanaka, T.; Moriwaki, H. Renin-angiotensin system inhibitors suppress azoxymethane-induced colonic preneoplastic lesions in C57BL/KsJ-db/db obese mice. *Biochem. Biophys. Res. Commun.* **2011**, *410*, 108–113.
38. Takahashi, M.; Wakabayashi, K. Gene mutations and altered gene expression in azoxymethane-induced colon carcinogenesis in rodents. *Cancer Sci.* **2004**, *95*, 475–480.
39. Chen, J.; Huang, X.F. The signal pathways in azoxymethane-induced colon cancer and preventive implications. *Cancer Biol. Ther.* **2009**, *8*, 1313–1317.
40. Reddy, B.S. Studies with the azoxymethane-rat preclinical model for assessing colon tumor development and chemoprevention. *Environ. Mol. Mutagenesis* **2004**, *44*, 26–35.
41. Raju, J. Azoxymethane-induced rat aberrant crypt foci: Relevance in studying chemoprevention of colon cancer. *World J. Gastroenterol.* **2008**, *14*, 6632–6635.
42. Ogawa, K.; Hara, T.; Shimizu, M.; Ninomiya, S.; Nagano, J.; Sakai, H.; Hoshi, M.; Ito, H.; Tsurumi, H.; Saito, K.; *et al.* Suppression of azoxymethane-induced colonic preneoplastic lesions in rats by 1-methyltryptophan, an inhibitor of indoleamine 2,3-dioxygenase. *Cancer Sci.* **2012**, *103*, 951–918.
43. Primer Blast. Available online: http://www.ncbi.nlm.nih.gov/tools/primer-blast/ (accessed on 12 July 2012).

Supplementary Information

Table S1. Primers sequences.

Target gene	Direction	Primer sequence (5'–3')
TNF-α	forward	AACACACGAGACGCTGAAGT
	reverse	TCCAGTGAGTTCCGAAAGCC
MCP-1	forward	TGGGCCTGTTGTTCACAGTT
	reverse	ACCTGCTGCTGGTGATTCTC
iNOS	forward	GTGGTGACAAGCACATTTGG
	reverse	GGCTGGACTTTTCACTCTGC
GPx	forward	TCCACCGTGTATGCCTTCTCC
	reverse	CCTGCTGTATCTGCGCACTGGA
CAT	forward	GAGGCAGTGTACTGCAAGTTCC
	reverse	GGGACAGTTCACAGGTATCTGC
GAPDH	forward	CCTTCATTGACCTCAACTACATGGT
	reverse	TCATTGTCATACCAGGAAATGAGCT

OPEN ACCESS Freely available online

PLOS ONE

Effects of Indoleamine 2,3-Dioxygenase Deficiency on High-Fat Diet-Induced Hepatic Inflammation

Junji Nagano[1], Masahito Shimizu[1*], Takeshi Hara[1], Yohei Shirakami[2], Takahiro Kochi[1], Nobuhiko Nakamura[1], Hirofumi Ohtaki[2], Hiroyasu Ito[2], Takuji Tanaka[3], Hisashi Tsurumi[1], Kuniaki Saito[4], Mitsuru Seishima[2], Hisataka Moriwaki[1]

1 Department of Internal Medicine, Gifu University Graduate School of Medicine, Gifu, Japan, **2** Department of Informative Clinical Medicine, Gifu University Graduate School of Medicine, Gifu, Japan, **3** Department of Tumor Pathology, Gifu University Graduate School of Medicine, Gifu, Japan, **4** Human Health Sciences, Graduate School of Medicine and Faculty of Medicine, Kyoto University, Kyoto, Japan

Abstract

Hepatic immune regulation is associated with the progression from simple steatosis to non-alcoholic steatohepatitis, a severe condition of inflamed fatty liver. Indoleamine 2,3-dioxygenase (IDO), an intracellular enzyme that mediates the catabolism of L-tryptophan to L-kynurenine, plays an important role in hepatic immune regulation. In the present study, we examined the effects of IDO gene silencing on high-fat diet (HFD)-induced liver inflammation and fibrosis in mice. After being fed a HFD for 26 weeks, the IDO-knockout (KO) mice showed a marked infiltration of inflammatory cells, especially macrophages and T lymphocytes, in the liver. The expression levels of F4/80, IFNγ, IL-1β, and IL-6 mRNA in the liver and the expression levels of F4/80 and TNF-α mRNA in the white adipose tissue were significantly increased in IDO-KO mice, although hepatic steatosis, the accumulation of intrahepatic triglycerides, and the amount of oxidative stress were lower than those in IDO-wild-type mice. IDO-KO mice also developed marked pericellular fibrosis in the liver, accumulated hepatic hydroxyproline, and exhibited increased expression levels of hepatic TGF-β1 mRNA. These findings suggest that IDO-KO renders the mice more susceptible to HFD-induced hepatic inflammation and fibrosis. Therefore, IDO may have a protective effect against hepatic fibrosis, at least in this HFD-induced liver injury model.

Citation: Nagano J, Shimizu M, Hara T, Shirakami Y, Kochi T, et al. (2013) Effects of Indoleamine 2,3-Dioxygenase Deficiency on High-Fat Diet-Induced Hepatic Inflammation. PLoS ONE 8(9): e73404. doi:10.1371/journal.pone.0073404

Editor: Rafael Aldabe, Centro de Investigación en Medicina Aplicada (CIMA), Spain

Received February 18, 2013; **Accepted** July 23, 2013; **Published** September 9, 2013

Funding: These authors have no support or funding to report.

Competing interests: The authors have declared that no competing interests exist.

* E-mail: shimim-gif@umin.ac.jp

Introduction

Non-alcoholic fatty liver disease (NAFLD), which is strongly associated with obesity and metabolic syndrome, is one of the most common causes of chronic liver disease worldwide. NAFLD includes a spectrum of disturbances that encompasses various degrees of liver damage ranging from non-alcoholic steatohepatitis (NASH), a severe condition of inflamed fatty liver that can progress to hepatic fibrosis, cirrhosis, or even hepatocellular carcinoma. The critical features of NASH, in addition to simple steatosis, include forms of hepatocellular degeneration such as ballooning and Mallory hyaline degeneration, mixed inflammatory cell infiltration, and the development of fibrosis [1,2]. Obesity is associated with chronic low-grade systemic inflammation, which contributes to the progression from hepatic steatosis to NASH [3]. Among various immune cells, T lymphocytes play a critical role in the induction of inflammation both in the liver and in white adipose tissue (WAT) [4,5]. Macrophage infiltration into WAT is also an early contributing event in the development of systemic inflammation because it is accompanied by tumor necrosis factor (TNF)-α production, a central mediator of the inflammatory response [6]. These reports, therefore, indicate that chronic inflammation plays a key role in the pathogenesis of NASH [7].

Indoleamine 2,3-dioxygenase (IDO), an intracellular enzyme that degrades the essential amino acid L-tryptophan along the L-kynurenine pathway, is induced during inflammation by several immune factors, including interferon (IFN) γ [8]. IDO is considered to exert powerful immunomodulatory effects, including the promotion of immune tolerance, because L-kynurenine and some other metabolites derived from tryptophan by IDO can inhibit T cell activation and proliferation while increasing immunosuppressive regulatory T-cell (Tregs) activity [9–11]. The liver is a special lymphoid organ and is thus particularly susceptible to injury as a result of the immune response, which is primarily mediated by T lymphocytes [12].

IDO is activated in infectious, autoimmune, and malignant diseases that involve cellular immune activation in various organs, including the liver [13]. In fact, upregulation of the IDO expression in the liver and increased serum IDO activity have been found in chronic hepatitis C patients [14,15]. The IDO expression is also enhanced in the liver and adipose tissue in obese individuals [16].

Several rodent studies have revealed the role of IDO in liver injury. In hepatitis B virus (HBV) transgenic mice, the IDO expression in hepatocytes is enhanced in mice with liver injury caused by HBV-specific cytotoxic T lymphocytes [17]. Inhibition of IDO activity exacerbates liver injury in both α-galactosylceramide- and carbon tetrachloride (CCl_4)-induced acute hepatitis models and is associated with the induction of TNF-α [18,19]. These reports suggest that IDO plays a critical role in the regulation of liver inflammation and that targeting IDO activity might be an effective strategy for attenuating acute liver injury. However, the role of IDO in steatosis-induced liver injury has not yet been clarified. In the present study, we examined the effects of IDO on high-fat diet (HFD)-induced liver steatosis and subsequent hepatic inflammation and fibrosis using IDO-deficient mice.

Materials and Methods

2.1 Animals and experimental procedure

This study was carried out in strict accordance with the recommendations of the Guide for the Care and Use of Laboratory Animals of Gifu University Life Science Research Center. The protocol was approved by the Committee on the Ethics of Animal Experiments of Gifu University (Permit Number: 24-65). All surgeries were performed under sodium pentobarbital anesthesia, and all efforts were made to minimize animal suffering. Five-week-old male IDO-wild-type (WT) mice and IDO-knockout (KO) mice with a C57BL/6J background were obtained from The Jackson Laboratory (Bar Harbor, ME, USA). HFD-60 (506.2 kcal/100 g) with 62.2% of the calories derived from fat was purchased from Oriental Yeast (Tokyo, Japan). The cholesterol content of the diet was 33.0 mg/100 g. After 1 week of acclimatization, 8 WT mice and 8 KO mice were given a pelleted HFD throughout the experiment (26 weeks) with free access to tap water and food. At the end of the experiment (32 weeks of age), all mice were sacrificed under sodium pentobarbital anesthesia and the livers were carefully removed.

2.2 Histopathological and immunohistochemical examinations

For all the experimental mice, 4 μm-thick sections of formalin-fixed and paraffin-embedded livers were stained with hematoxylin & eosin (H&E) for conventional histopathology or with Sirius Red stain to determine the presence of liver fibrosis. The histological features of the livers were evaluated using the NAFLD activity score (NAS) system [20]. The computer-assisted quantitative analyses of hepatic fibrosis development were carried out using the BZ-Analyzer-II software program (KEYENCE, Osaka, Japan) [21,22].

In order to evaluate the infiltration of inflammatory cells in the liver, immunohistochemical staining for Mac-1 (a macrophage marker), CD3 (a T-cell marker), and NIMP-R14 (a neutrophil marker) of paraffin-embedded sections was performed using the linked streptavidin-biotin method. Rat monoclonal anti-Mac-1 antibody (MAB1387Z, 1:50 dilution) was purchased from Chemicon Iuternational (Temecula, CA, USA). Rabbit polyclonal anti-CD3 (ab5690, 1:100 dilution) antibodies and rat monoclonal anti-neutrophil antibody (NIMP-R14, ab2557, 1:50 dilution) were obtained from Abcam (Cambridge, MA, USA). On the Mac-1-, CD3-, and NIMP-R14-immunostained sections, the inflammatory cells that intensively reacted to these antibodies were counted and the data are expressed as the percentage of total inflammatory cells in the liver. A positive cell index (%) was determined by counting at least 500 cells in a section from each mouse.

2.3 Hepatic hydroxyproline analysis

The hepatic hydroxyproline content (μmol/g wet liver) was quantified colorimetrically in duplicate samples from approximately 200mg of the wet-weight liver tissues, as described previously [22].

2.4 RNA extraction and quantitative real-time RT-PCR analysis

Total RNA was isolated from the livers and adipose tissue of the mice using the RNeasy Mini Kit and RNeasy Lipid Tissue Mini Kit (Qiagen, Hilden, Germany), respectively [21]. cDNA was amplified from 0.5 μg of total RNA using the SuperScript III First-Strand Synthesis System (Invitrogen, Carlsbad, CA, USA). A quantitative real-time reverse transcription-PCR (RT-PCR) analysis was performed using specific primers that amplify F4/80, IFNγ, interleukin (IL)-1β, IL-6, TNF-α, superoxide dismutase (SOD)-1, SOD-2, glutathione peroxidase (GPx), transforming growth factor (TGF)-β1, glyceraldehyde-3-phosphate dehydrogenase (GAPDH), and the ribosomal protein large P0 (RPLP0) genes. The sequences of the primers for these genes, which were obtained from Universal ProbeLibrary Assay Design Center (Roche, Indianapolis, IN, USA), are shown in Table 1. The analysis to quantify the expression levels of tryptophan 2,3-dioxygenase (TDO) was performed using TaqMan Gene Expression Assays (Applied Biosystems, Foster City, CA, USA) and TOYOBO Real-time PCR Master Mix (TOYOBO, Osaka, Japan), as described previously [23]. Each sample was analyzed on a LightCycler Nano (Roche) with FastStart Essential DNA Green Master (Roche). The parallel amplification of GAPDH and RPLP0 was used as the internal control for liver and adipose tissue, respectively.

2.5 Clinical chemistry

The serum levels of alanine aminotransferase (ALT) were measured using a standard clinical automatic analyzer (type 7180; Hitachi, Tokyo, Japan).

Table 1. Primer sequences.

Gene	Primer sequence
SOD1	F 5'-CAGGACCTCATTTTAATCCTCAC-3'
	R 5'-TGCCCAGGTCTCCAACAT-3'
SOD2	F 5'-TGCTCTAATCAGGACCCATTG-3'
	R 5'-GTAGTAAGCGTGCTCCCACAC-3'
GPX	F 5'-TTTCCCGTGCAATCAGTTC-3'
	R 5'-TCGGACGTACTTGAGGGAAT-3'
F4/80	F 5'-ACAAGACTGACAACCAGACGG-3'
	R 5'-TAGCATCCAGAAGAAGCAGGCGA-3'
IFNγ	F 5'-AGCAACAGCAAGGCGAAAAAG-3'
	R 5'-CGCTTCCTGAGGCTGGATTC-3'
IL-1β	F 5'-CAAGCAACGACAAAATACCTGTG-3'
	R 5'-AGACAAACCGTTTTTCCATCTTCT-3'
IL-6	F 5'-CCGGAGAGGAGACTTCACAGAG-3'
	R 5'-CTGCAAGTGCATCATCGTTGTT-3'
TNF-α	F 5'-TGGCCCAGACCCTCACACTCAG-3'
	R 5'-ACCCATCGGCTGGCACCACT-3'
TGF-β1	F 5'-ACCGGAGAGCCCTGGATACCA-3'
	R 5'-TATAGGGGCAGGGTCCCAGACA-3'
RPLP0	F 5'-ACTGCTCTAGCACCGGAGAAG-3'
	R 5'-CTCCCACCTTGTCTCCAGTC-3'
GAPDH	F 5'-GACATCAAGAAGGTGGTGAAGCAG-3'
	R 5'-ATACCAGGAAATGAGCTTGACAAA-3'

doi: 10.1371/journal.pone.0073404.t001

2.6 Oxidative stress analysis

The serum hydroperoxide levels, one of the markers of oxidative stress, were determined using the derivatives of reactive oxygen metabolites (d-ROM) test (FREE Carpe Diem; Diacron s.r.l., Grosseto, Italy), according to the manufacturer's protocol.

2.7 Determination of the enzymatic activity of IDO

The IDO activity level in the serum was determined by calculating the ratio of the L-kynurenine/L-tryptophan concentrations [23]. Serum samples were deproteinized with 3% perchloric acid. Following centrifugation, aliquots of supernatant were collected to determine the concentrations of L-tryptophan and L-kynurenine using HPLC, as described previously [18].

2.8 Hepatic lipid analysis

After total lipids were extracted from the frozen livers (approximately 200 mg), the triglyceride levels were measured using the triglyceride E-test kit (Wako, Osaka, Japan) [21].

2.9 Statistical analysis

The data are expressed as the mean ± SD. Statistical significance of the difference between mean values was evaluated using the Mann-Whitney *U* test. Significance was defined as a *P* value less than 0.05.

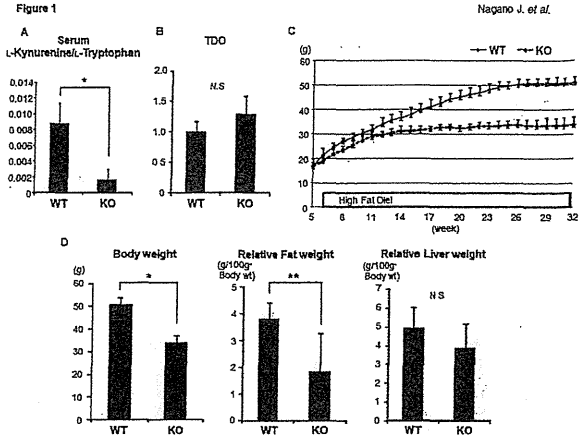

Figure 1. Effects of IDO deficiency on the serum L-kynurenine/L-tryptophan ratio, the expression levels of TDO in the liver, the growth curve, and the body, liver, and fat weights of the experimental mice. (A) The functional IDO activity level was determined by measuring the concentrations of L-kynurenine and L-tryptophan using HPLC. The L-kynurenine/L-tryptophan ratio indicates the IDO activity. (B) Total RNA was isolated from the livers of the experimental mice, and the expression levels of TDO mRNA were examined using quantitative real-time RT-PCR with specific primers. (C) The growth curve of the experimental mice. The body weights of all mice were measured once a week during the experiment. (D) The body weights and relative weights of the adipose tissues and livers of the experimental mice at the termination of the study. The values are expressed as the mean ± SD. * $P < 0.001$, ** $P < 0.05$.

doi: 10.1371/journal.pone.0073404.g001

Results

3.1 General observations

We initially examined the enzymatic activity of IDO in the serum of the experimental mice by measuring the concentrations of L-kynurenine and L-tryptophan. The L-kynurenine/L-tryptophan ratios in serum of the IDO-KO mice were significantly lower than those in the serum of the IDO-WT mice (Figure 1A, $P < 0.001$), indicating that IDO activity was clearly inhibited in the IDO-KO mice. TDO, a hepatic enzyme that catalyses the first step of tryptophan degradation, was expressed in the liver in both the IDO-WT mice and the IDO-KO mice; however, IDO deficiency did not have a significant effect on the TDO mRNA expression (Figure 1B). Figure 1C shows the growth curves of the mice during this experiment. The body weight gain of the IDO-KO mice was smaller than that of the IDO-WT mice. At the end of the experiment, the body weights (Figure 1D, $P < 0.001$) and the relative weights of the adipose tissues of the IDO-KO mice (Figure 1D, $P < 0.05$) were also significantly lower than those of the IDO-WT mice.

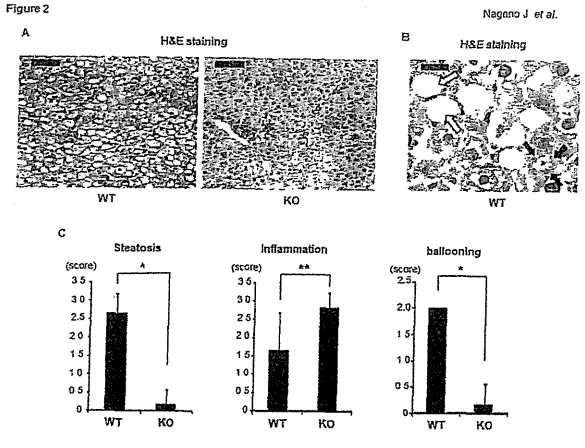

Figure 2. Effects of IDO deficiency on hepatic histopathology in the experimental mice. (A) and (B) H&E staining of liver sections from the experimental mice. (A) Representative photomicrographs of the liver sections of the IDO-WT mice and IDO-KO mice (low-power field). Black bar: 100 μm. (B) An enlarged photo (high-power field) of the liver sections from the IDO-WT mice. Ballooned hepatocytes (indicated by white arrows) and Mallory-Denk bodies (indicated by black arrows) were observed. Black bar: 20 μm. (C) The presence of NAS (steatosis, inflammation, and ballooning) was determined based on the histopathological analysis. The values are expressed as the mean ± SD. * P <0.001, ** P <0.05.

doi: 10.1371/journal.pone.0073404.g002

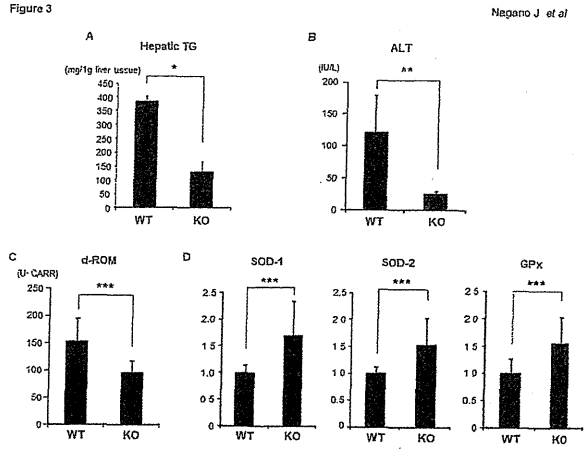

Figure 3. Effects of IDO deficiency on intrahepatic triglycerides, the serum ALT levels, and oxidative stress in the experimental mice. (A) Hepatic lipids were extracted from the frozen livers of the experimental mice, and the triglyceride levels were measured. (B) At sacrifice, blood samples were collected and the serum levels of ALT were assayed. (C) The hydroperoxide levels in the serum at the end of the experiment were determined using the d-ROM test. (D) Total RNA was isolated from the livers of the experimental mice, and the expression levels of SOD-1, SOD-2, and GPx mRNA were examined using quantitative real-time RT-PCR with specific primers. The values are expressed as the mean ± SD. * P <0.001, ** P <0.01, *** P <0.05.

doi: 10.1371/journal.pone.0073404.g003

3.2 Effects of IDO deficiency on hepatic histopathology in the experimental mice

The H&E staining results of the livers of the IDO-KO mice and IDO-WT mice after 26 weeks of being fed the HFD are presented in Figure 2A and B. The infiltration of inflammatory cells was markedly increased in the livers of the IDO-KO mice, and the NAS inflammation scores were significantly higher than those in the IDO-WT mice (Figure 2C, $P < 0.05$). Interestingly, the hepatic steatosis and ballooning degeneration of hepatocytes were lower in the IDO-KO mice than in the IDO-WT mice at this experimental time point (Figure 2C, $P < 0.001$). In addition to the ballooned hepatocytes, Mallory-Denk bodies, which are a recognized feature of alcoholic hepatitis and NASH [24], were also observed in the liver of IDO-WT mice (Figure 2B).

3.3 Effects of IDO deficiency on the intrahepatic triglyceride levels, the serum ALT levels, and oxidative stress in the experimental mice

The histological findings were consistent with the measured intrahepatic triglyceride contents: the levels of triglycerides in the livers of the IDO-KO mice were significantly lower than those in the livers of the IDO-WT mice (Figure 3A, $P < 0.001$). The serum levels of ALT in the IDO-KO mice were also significantly decreased relative to those in the IDO-WT mice (Figure 3B, $P < 0.01$). In addition, the serum d-ROM levels, which reflect the serum hydroperoxide levels, were significantly lower in the IDO-KO mice than in the IDO-WT mice (Figure 3C, $P < 0.05$). Compared to the IDO-WT mice, there were also significant increases in the expression levels of SOD-1, SOD-2, and GPx mRNA, which encode antioxidant enzymes, in the livers of the IDO-KO mice (Figure 3D, $P < 0.05$). These findings indicate that hepatic triglyceride accumulation and oxidative stress are reduced, while antioxidant activity is increased, in mice lacking the IDO gene.

3.4 Effects of IDO deficiency on inflammation in the livers and WAT of the experimental mice

We next examined the expression levels of inflammatory mediators that are implicated in the progression of fatty liver to NASH [7] in the experimental mice. A quantitative real-time RT-PCR analysis revealed that the expression levels of F4/80, a marker of macrophages, were significantly increased in the livers of the IDO-KO mice in comparison to those observed in the livers of the IDO-WT mice (Figure 4A, $P < 0.01$). There were also significant increases in the expression levels of inflammatory mediators, including IFNγ, IL-1β, and IL-6 mRNA, in the livers of the IDO-KO mice compared to those observed in the livers of the IDO-WT mice (Figure 4A, $P < 0.05$). The expression levels of TNF-α mRNA were also higher in the livers of the IDO-KO mice than in the livers of the IDO-WT mice;

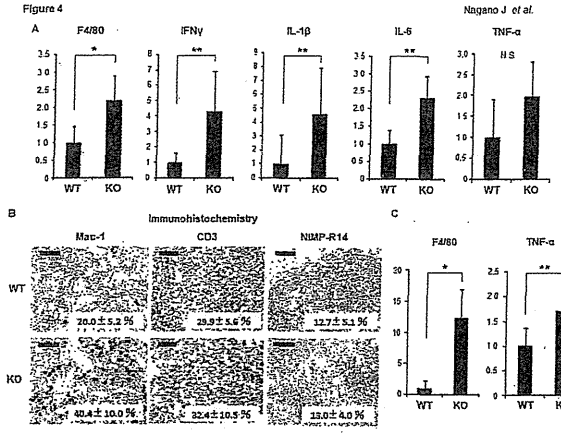

Figure 4. Effects of IDO deficiency on the inflammation in the liver and white adipose tissue of the experimental mice. (A) The expression levels of F4/80, IFNγ, IL-1β, IL-6, and TNF-α mRNA in the livers of the experimental mice. (B) The results of the immunohistochemical analyses of Mac-1, CD3, and NIMP-R14 in the livers of the experimental mice. A positive cell index (%) was shown in each photo. Black bar: 50 μm. (C) The expression levels of F4/80 and TNF-α mRNA in the WAT of the experimental mice. Total RNA was isolated from the livers (A) and WAT (C) of the experimental mice, and the expression levels of each mRNA were examined using quantitative real-time RT-PCR with specific primers. The expression levels of GAPDH mRNA and RPLP0 mRNA were used as internal controls for the liver and WAT, respectively. The values are expressed as the mean ± SD. * P <0.01, ** P <0.05.

doi: 10.1371/journal.pone.0073404.g004

however, the difference was insignificant (Figure 4A). Furthermore, the immunohistochemical analyses demonstrated that the inflammatory cells that had infiltrated into the livers of the IDO-KO mice positively reacted with either the anti-Mac-1(40.4 ± 10.0%) or anti-CD3 (32.4 ± 10.5%) antibodies. On the other hand, the infiltration of neutrophils (13.0 ± 4.0%) was low compared to that of macrophages and T-cells. These findings suggest that macrophages and T lymphocytes were the predominantly increased cell populations in the livers of the IDO-KO mice. The infiltration of Mac-1 positive cells in the livers of IDO-KO mice (40.4 ± 10.0%) was high compared to that of IDO-WT mice (20.0 ± 5.2%) (Figure 4B, $P < 0.05$), and this is consistent with the results of RT-PCR analysis showing the increased levels of F4/80 mRNA in the livers of IDO-KO mice (Figure 4A).

Moreover, as shown in Figure 4C, the expression levels of F4/80 ($P < 0.01$) and TNF-α($P < 0.05$) mRNA in WAT were both significantly increased in the IDO-KO mice compared to those observed in the IDO-WT mice, indicating that inflammation is augmented in WAT, in addition to the liver, in the IDO-KO mice [24].

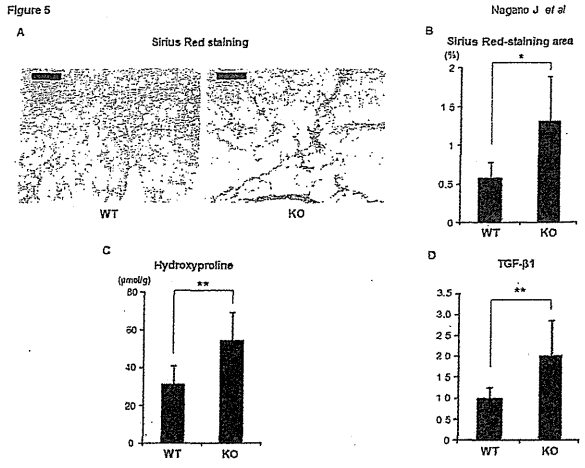

Figure 5. Effects of IDO deficiency on the hepatic fibrosis in the experimental mice. (A) Representative photomicrographs of liver sections stained with Sirius Red to show fibrosis. Black bar: 100 μm. (B) The Sirius Red-stained images of fibrosis were analyzed using a BZ-9000 fluorescence microscope, and the fibrotic area was measured using a BZ-Analyzer-II. (C) The hepatic hydroxyproline contents were quantified colorimetrically. (D) Total RNA was isolated from the livers of the experimental mice, and the expression levels of TGF-β1 mRNA were examined using quantitative real-time RT-PCR with specific primers. The values are expressed as the mean ± SD. * P <0.01, ** P <0.05.

doi: 10.1371/journal.pone.0073404.g005

3.5 Effects of IDO deficiency on hepatic fibrosis in the experimental mice

We next examined whether IDO deficiency has an effect on the development of steatosis-induced hepatic fibrosis. An examination of Sirius Red-stained sections indicated that, compared to the IDO-WT mice, the IDO-KO mice markedly developed pericellular fibrosis in the liver (Figure 5A and B, $P < 0.01$). Similar findings were observed in the measured hepatic hydroxyproline contents: the IDO-KO mice showed a significant increase in the amount of hydroxyproline observed in the liver (Figure 5C, $P < 0.05$). The expression levels of TGF-β1 mRNA, a central regulator of chronic liver disease contributing to fibrogenesis through inflammation [25], were also remarkably elevated in the livers of the IDO-KO mice compared to those observed in the livers of the IDO-WT mice (Figure 5D, $P < 0.05$). These findings may indicate that IDO-KO mice are susceptible to the development of steatosis-induced hepatic fibrosis.

Discussion

The results of the present study indicate that HFD-induced hepatic inflammation and fibrosis are significantly aggravated in IDO-KO mice, although the level of hepatic steatosis and amount of oxidative stress were lower compared to those in IDO-WT mice. Therefore, IDO deficiency is critically involved in

the acceleration of hepatic inflammation observed in the present study.

IDO is a rate-limiting enzyme that can degrade tryptophan via the kynurenine pathway. Because the IDO expression and its enzymatic activity, which are tightly controlled by several immune mediators such as IFNγ, play a key role in the suppression of the immune response [8–11], inhibiting the expression and activity of IDO might promote inflammatory signaling. Therefore, based on our present results, we consider that IDO-deficient mice are more susceptible to the induction of inflammation by HFD. Our results are consistent with those of recent reports showing that the inhibition of the enzymatic activity of IDO significantly exacerbated liver injury in α-galactosylceramide (α-GalCer)- and CCl_4-induced acute hepatitis animal models via the upregulation of IL-6 and TNF-α [18,19]. When the IDO-KO mice were treated with α-GalCer, the production of TNF-α from the infiltrating macrophages in the liver was significantly accelerated, and thus led to the development of severe hepatitis [18]. Therefore, in the present study, the increase in the number of hepatic macrophages might have been critically involved in the exacerbation of HFD-induced hepatic inflammation in the IDO-KO mice. These reports [18,19], together with the results of the present study, suggest that IDO may play a critical role in suppressing excess induction and progression of inflammation in the liver.

Innate immune cells, including Kupffer cells, natural killer T cells, and natural killer cells, play important roles in the excessive production of hepatic T helper 1 cytokines, which is associated with the development of steatohepatitis [4]. The regulation of the immune response by IDO is predominantly based on the ability of IDO to suppress the activation of lymphocytes [9–11]. An increased IDO activity inhibits proliferation and induces apoptosis in T cells and natural killer cells via tryptophan depletion and the production of toxic tryptophan metabolites [9]. In addition, recent studies have revealed that IDO inhibits T cell activation by driving the development of Tregs [10,11]. Tregs, which are actively engaged in the negative control of a variety of immune responses, are recognized as being one of the key players in hepatic immune regulation [26]. HFD-induced steatosis in mice is associated with the depletion of hepatic Tregs and leads to upregulation of the inflammatory pathway [27]. Therefore, an IDO deficiency may increase T cell activation, either directly or indirectly, by suppressing Tregs and thus contributed to a worsening of hepatic inflammation in the present study.

Obesity is associated with systemic low-grade inflammation and immune activation [5,6]. One clinical trial reported that activation of IDO is associated with reduced plasma tryptophan levels in obese patients [28]. IDO is also overexpressed in the liver and adipose tissue in obese subjects [16]. These reports indicate that the overexpression and activation of IDO are implicated in chronic immune activation in obese individuals. T cell infiltration into WAT and subsequent recruitment and activation of macrophages can induce TNF-α production, which is associated with the development of systemic inflammation [5,6]. The present study showed that the expression levels of F4/80 and TNF-α mRNA in WAT are elevated in IDO-KO mice compared to those observed in IDO-WT mice when the mice are fed an HFD, indicating that inflammation of WAT induced by HFD is worsened in IDO deficiency mice. Therefore, our findings suggest that IDO might have the ability to attenuate overactive immune responses caused by obesity in WAT in addition to the liver.

There are some possible limitations associated with the present study. For instance, a recent study demonstrated that neither the overexpression of IDO nor inhibition of its enzymatic activity affected the lipid accumulation in the liver, although the combination of L-tryptophan treatment and a high fat and high fructose diet exacerbated the hepatic steatosis [29]. Therefore, further experiments will be required to clarify the role of IDO and the L-kynurenine/L-tryptophan pathway in the development of hepatic steatosis. Furthermore, after 26 weeks of being fed the HFD, the IDO-KO mice showed lower steatosis and oxidative stress than the IDO-WT mice. The hepatocyte ballooning, which indicates hepatocyte injury, was also decreased in IDO-KO mice compared to IDO-WT mice. These findings seem paradoxical given the enhanced inflammation and fibrosis in IDO-KO mice in response to the HFD. A possible explanation might be that the liver inflammation proceeded earlier in IDO-KO mice, in a similar manner to NAFLD in the clinical setting, where many cases with NAFLD show the disappearance of steatosis during its natural history, while exhibiting severe fibrosis and cirrhosis in the late stages [30,31]. In order to verify this possibility, time course studies that evaluate the levels of hepatic injury, steatosis, and inflammation caused by HFD in the early phase should be conducted. In addition, a recent study revealed that hepatic fat deposits were broken down to provide energy for fibrogenesis in a CCl_4-treated mouse model [32]. Such a mechanism might have also been active in our HFD-fed IDO-KO mice, but again, further experiments will be required to confirm this hypothesis.

In conclusion, we herein demonstrated that IDO deficiency worsens hepatic and WAT inflammation in mice fed an HFD. Our findings suggest that regulation of the IDO-mediated immune response might be an interesting strategy for managing steatosis-related hepatic injury.

Author Contributions

Performed the experiments: JN YS TK NN HO. Analyzed the data: JN MS TT. Wrote the manuscript: JN MS TH HI TT HT KS MS HM.

References

1. Angulo P (2002) Nonalcoholic fatty liver disease. N Engl J Med 346: 1221-1231. doi:10.1056/NEJMra011775. PubMed: 11961152.
2. Farrell GC, Larter CZ (2006) Nonalcoholic fatty liver disease: from steatosis to cirrhosis. Hepatology 43: S99-S112. doi:10.1002/hep.20973. PubMed: 16447287.
3. Cusi K (2012) Role of obesity and lipotoxicity in the development of nonalcoholic steatohepatitis: pathophysiology and clinical implications. Gastroenterology 142: 711-725 e716 doi:10.1053/j.gastro.2012.02.003. PubMed: 22326434.
4. Zhan YT, An W (2010) Roles of liver innate immune cells in nonalcoholic fatty liver disease. World J Gastroenterol 16: 4652-4660. doi:10.3748/wjg.v16.i37.4652. PubMed: 20872965.
5. Chatzigeorgiou A, Karalis KP, Bornstein SR, Chavakis T (2012) Lymphocytes in obesity-related adipose tissue inflammation. Diabetologia 55: 2583-2592. doi:10.1007/s00125-012-2607-0. PubMed: 22733483.
6. Weisberg SP, McCann D, Desai M, Rosenbaum M, Leibel RL et al. (2003) Obesity is associated with macrophage accumulation in adipose tissue. J Clin Invest 112: 1796-1808. doi:10.1172/JCI19246. PubMed: 14679176.
7. Fujii H, Kawada N (2012) Inflammation and fibrogenesis in steatohepatitis. J Gastroenterol 47: 215-225. doi:10.1007/s00535-012-0527-x. PubMed: 22310735.
8. Fallarino F, Grohmann U, Puccetti P (2012) Indoleamine 2,3-dioxygenase: from catalyst to signaling function. Eur J Immunol 42: 1932-1937. doi:10.1002/eji.201242572. PubMed: 22865044.
9. Frumento G, Rotondo R, Tonetti M, Damonte G, Benatti U et al. (2002) Tryptophan-derived catabolites are responsible for inhibition of T and natural killer cell proliferation induced by indoleamine 2,3-dioxygenase. J Exp Med 196: 459-468. doi:10.1084/jem.20020121. PubMed: 12186838.
10. Mellor AL, Munn DH (2004) IDO expression by dendritic cells: tolerance and tryptophan catabolism. Nat Rev Immunol 4: 762-774. doi:10.1038/nri1457. PubMed: 15459668.
11. Munn DH (2011) Indoleamine 2,3-dioxygenase, Tregs and cancer. Curr Med Chem 18: 2240-2246. doi:10.2174/092986711795656045. PubMed: 21517755.
12. Dienes HP, Drebber U (2010) Pathology of immune-mediated liver injury. Dig Dis 28: 57-62. doi:10.1159/000282065. PubMed: 20460891.
13. Schröcksnadel K, Wirleitner B, Winkler C, Fuchs D (2006) Monitoring tryptophan metabolism in chronic immune activation. Clin Chim Acta 364: 82-90. doi:10.1016/j.cca.2005.06.013. PubMed: 16139256.
14. Larrea E, Riezu-Boj JI, Gil-Guerrero L, Casares N, Aldabe R et al. (2007) Upregulation of indoleamine 2,3-dioxygenase in hepatitis C virus infection. J Virol 81: 3662-3666. doi:10.1128/JVI.02248-06. PubMed: 17229698.
15. Higashitani K, Kanto T, Kuroda S, Yoshio S, Matsubara T et al. (2012) Association of enhanced activity of indoleamine 2,3-dioxygenase in dendritic cells with the induction of regulatory T cells in chronic hepatitis C infection. J Gastroenterol, 48: 660–70. PubMed: 22976933.
16. Wolowczuk I, Hennart B, Leloire A, Bessede A, Soichot M et al. (2012) Tryptophan metabolism activation by indoleamine 2,3-dioxygenase in adipose tissue of obese women: an attempt to maintain immune homeostasis and vascular tone. Am J Physiol Regul Integr Comp Physiol 303: R135-R143. doi:10.1152/ajpregu.00373.2011. PubMed: 22592557.
17. Iwamoto N, Ito H, Ando K, Ishikawa T, Hara A et al. (2009) Upregulation of indoleamine 2,3-dioxygenase in hepatocyte during acute hepatitis caused by hepatitis B virus-specific cytotoxic T lymphocytes in vivo. Liver Int 29: 277-283. doi:10.1111/j.1478-3231.2008.01748.x. PubMed: 18397228.
18. Ito H, Hoshi M, Ohtaki H, Taguchi A, Ando K et al. (2010) Ability of IDO to attenuate liver injury in alpha-galactosylceramide-induced hepatitis model. J Immunol 185: 4554-4560. doi:10.4049/jimmunol.0904173. PubMed: 20844202.
19. Li D, Cai H, Hou M, Fu D, Ma Y et al. (2012) Effects of indoleamine 2,3-dioxygenases in carbon tetrachloride-induced hepatitis model of rats. Cell Biochem Funct 30: 309-314. doi:10.1002/cbf.2803. PubMed: 22249930.
20. Kleiner DE, Brunt EM, Van Natta M, Behling C, Contos MJ et al. (2005) Design and validation of a histological scoring system for nonalcoholic fatty liver disease. Hepatology 41: 1313-1321. doi:10.1002/hep.20701. PubMed: 15915461.
21. Terakura D, Shimizu M, Iwasa J, Baba A, Kochi T et al. (2012) Preventive effects of branched-chain amino acid supplementation on the spontaneous development of hepatic preneoplastic lesions in C57BL/KsJ-db/db obese mice. Carcinogenesis, 33: 2499–506. PubMed: 23027617.
22. Yasuda Y, Shimizu M, Sakai H, Iwasa J, Kubota M et al. (2009) (-)-Epigallocatechin gallate prevents carbon tetrachloride-induced rat hepatic fibrosis by inhibiting the expression of the PDGFRbeta and IGF-1R. Chem Biol Interact 182: 159-164. doi:10.1016/j.cbi.2009.07.015. PubMed: 19646978.
23. Ogawa K, Hara T, Shimizu M, Ninomiya S, Nagano J et al. (2012) Suppression of azoxymethane-induced colonic preneoplastic lesions in rats by 1-methyltryptophan, an inhibitor of indoleamine 2,3-dioxygenase. Cancer Sci 103: 951-958. doi:10.1111/j.1349-7006.2012.02237.x. PubMed: 22320717.
24. Machado MV, Cortez-Pinto H (2011) Cell death and nonalcoholic steatohepatitis: where is ballooning relevant? Expert Rev Gastroenterol Hepatol 5: 213-222. doi:10.1586/egh.11.16. PubMed: 21476916.
25. Dooley S, ten Dijke P (2012) TGF-beta in progression of liver disease. Cell Tissue Res 347: 245-256. doi:10.1007/s00441-011-1246-y. PubMed: 22006249.
26. Chang KM (2005) Regulatory T cells and the liver: a new piece of the puzzle. Hepatology 41: 700-702. doi:10.1002/hep.20678. PubMed: 15789365.
27. Ma X, Hua J, Mohamood AR, Hamad AR, Ravi R et al. (2007) A high-fat diet and regulatory T cells influence susceptibility to endotoxin-induced liver injury. Hepatology 46: 1519-1529. doi:10.1002/hep.21823. PubMed: 17661402.
28. Brandacher G, Winkler C, Aigner F, Schwelberger H, Schroecksnadel K et al. (2006) Bariatric surgery cannot prevent tryptophan depletion due to chronic immune activation in morbidly obese patients. Obes Surg 16: 541-548. doi:10.1381/096089206776945066. PubMed: 16687019.
29. Osawa Y, Kanamori H, Seki E, Hoshi M, Ohtaki H et al. (2011) L-tryptophan-mediated enhancement of susceptibility to nonalcoholic fatty liver disease is dependent on the mammalian target of rapamycin. J Biol Chem 286: 34800-34808. doi:10.1074/jbc.M111.235473. PubMed: 21841000.
30. Maheshwari A, Thuluvath PJ (2006) Cryptogenic cirrhosis and NAFLD: are they related? Am J Gastroenterol 101: 664-668. doi:10.1111/j.1572-0241.2006.00478.x. PubMed: 16464222.
31. Caldwell SH, Lee VD, Kleiner DE, Al-Osaimi AM, Argo CK et al. (2009) NASH and cryptogenic cirrhosis: a histological analysis. Ann Hepatol 8: 346-352. PubMed: 20009134.
32. Hernández-Gea V, Ghiassi-Nejad Z, Rozenfeld R, Gordon R, Fiel MI et al. (2012) Autophagy releases lipid that promotes fibrogenesis by activated hepatic stellate cells in mice and in human tissues. Gastroenterology 142: 938-946. doi:10.1053/j.gastro.2011.12.044. PubMed: 22240484.